Scanning-Tunneling-Microscopy Study of Distortion and Instability of Inclined Flux-Line-Lattice Structures in the Anisotropic Superconductor $2H$-$NbSe_2$

H. F. Hess, C. A. Murray, and J. V. Waszczak
AT&T Bell Laboratories, Murray Hill, New Jersey 07974
(Received 27 July 1992)

The tilted vortex lattice on the surface of $2H$-$NbSe_2$ is investigated with a scanning-tunneling microscope at magnetic fields, such that the vortex separation is comparable to or smaller than the magnetic penetration depth. The basis vectors show a distortion roughly consistent with bulk anisotropic London theory; however, their angular orientation with respect to the tilt direction differs by 30° from that predicted. At field inclinations greater than 80° from the c axis, we find two instabilities into ordered, buckled rows of vortices, followed by a disordering transition.

PACS numbers: 74.60.Ec, 61.16.Di, 74.60.Ge

The availability of good single-crystal high-T_c superconducting samples has recently generated interest in the structure and dynamics of Abrikosov flux-line lattices in highly anisotropic type-II materials. In particular for fields tilted away from the c axis exotic lattice structures have been predicted. In low fields, such that the nearest-neighbor distance is much greater than the penetration depth, vortex chains have been proposed [1] and observed [2,3] with Bitter decoration experiments. In $Bi_2Sr_2CaCu_2O_8$ (effective-mass anisotropy $m_c/m_a=3600$) vortex chains with interspersed isotropic vortex lattices are seen [2], while those on $YBa_2Cu_3O_7$ ($m_c/m_a=50$) appear to have simple uncorrelated vortex chain structures [3] along the field direction. At higher fields ($H_{c1}\ll H\ll H_{c2}$), different well-defined distortions of the flux-line lattice have been proposed on the basis of anisotropic London theory [4] and anisotropic Landau Ginzberg theory [5], yet only one neutron scattering experiment has begun to probe this regime [6].

In this Letter we report comprehensive scanning-tunneling-microscope (STM) measurements of the flux-line-lattice structure at these higher fields for the conventional anisotropic layered superconductor $2H$-$NbSe_2$. We find a striking contrast between our results and the structures recently observed in the low field, high-T_c cases. Our 0.3-cm×50-μm-thick $2H$-$NbSe_2$ sample has a superconducting transition at 7.2 K, a mass ratio [7] m_c/m_a of roughly 11, and an in-plane penetration depth [8] λ of 2000 Å. It is considered a clean superconductor that also supports a charge-density-wave transition at 33 K. With STM we can study a larger range of intermediate fields $H_{c1}=0.1\ll H\ll H_{c2}=45$ kG compared to that available by the Bitter technique, so that we can make a comparison between the strongly interacting (vortex separation $a_0\leq\lambda$) versus weakly interacting ($a_0>\lambda$) regimes. Currently, the STM scans are limited to a region of roughly 4 μm^2 square (≤ 500 vortices), and take over an hour to complete. We find the following: (i) distortions of the vortex lattice structure consistent with those predicted by second-order uniaxial anisotropic theories [4,5] with a slight (30–50)% disagreement in the ratio m_c/m_a compared to that determined by the anisotropy of H_{c2} [7]; however, (ii) the basis vectors of the vortex lattice rotate to exactly 30° off from that predicted as the lowest-energy structure by the same theory; and (iii) hitherto unobserved structural instabilities as the tilt angle is increased beyond $\theta=80°$ with at least two distinct buckling phases with 3×1 and 2×1 ordered superlattice structures, followed by a probable disordering transition.

The vortices are imaged with STM [9] by tunneling with a tip-sample bias voltage set just above the energy gap value of 1.1 meV and recording the differential conductance $dI/dV(x,y)$ on the surface. A three-axis solenoid applies the magnetic field H_a at an angle θ with respect to the c axis, with a planar component that is at an angle φ away from the $NbSe_2$ crystalline band-structure ΓM direction. (ΓM corresponds to the charge-density-wave vector of this compound and is 30° rotated from the sixfold crystalline a axis.) About 80 different field configurations were explored at four different fields [$H_a=0.5$, 1.0, 2.25, and 5.0 kG, where the Abrikosov lattice spacing, $a_0=(2\Phi_0/\sqrt{3}B)^{1/2}$ is about 1.1λ, 0.77λ, 0.52λ, and 0.35λ], ten different values of θ and two different planar projections ($\varphi=+7°$ and $-21°$). Each field configuration was separately field cooled from T_c to 200 mK and all images were taken on the same position on the sample.

The essence of the data can be seen in the STM images of Fig. 1. Here the magnitude of H_a is constant at 2.25 kG and the tilt angle θ is indicated. For $\mathbf{B}\|\mathbf{c}$ ($\theta=0°$) a hexagonal Abrikosov flux-line lattice is observed. The angular orientation of the flux-line lattice is locked to the atomic crystal, so that the nearest-neighbor direction is identical to the crystalline **a** direction. This image is used to remove any residual linear x,y scale distortions of the STM to better than 1% accuracy (under the assumption that this lattice has a perfect hexagonal structure). For tilt angle θ values of 60° and 76° (Fig. 1) an increase of the lattice spacing on the sample surface is observed with increasing θ in the direction of the applied field. These surface images reflect the vortex density that follows the vertical component of the magnetic field B_Z (accurate to about 5 G).

To determine the vortex lattice basis vectors, the STM

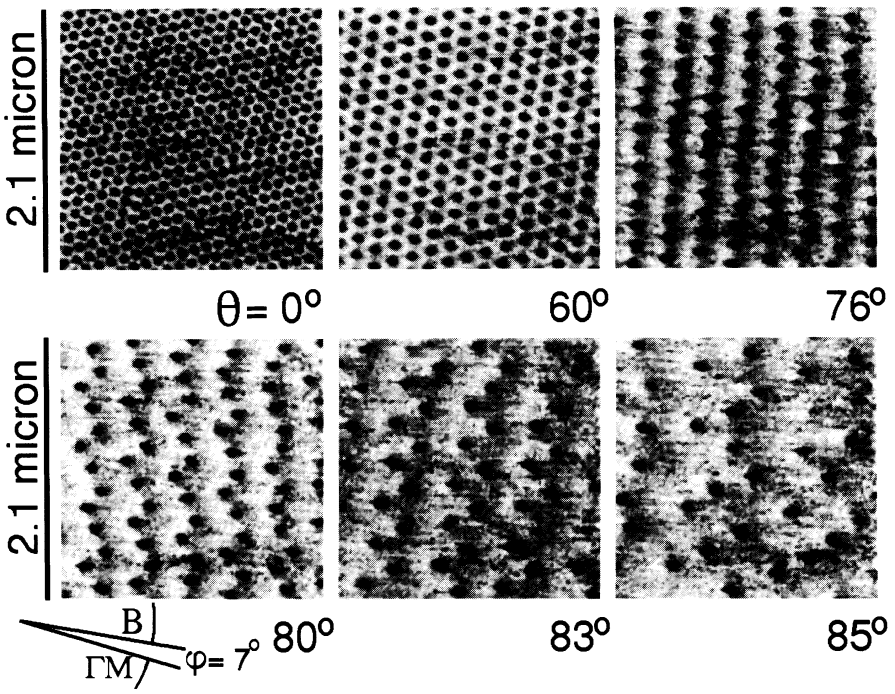

FIG. 1. STM conductance images dI/dV $(x,y,V=1.3$ mV) showing vortex locations on the surface of $2H$-$NbSe_2$ at $\theta=0°$, 60°, and 76° (top row) and 80°, 83°, and 85° (bottom row) where the buckled and disordered phases are evident. The directions of ΓM and the in-plane projection of B are indicated. The applied field is 2.25 kG.

images are Gaussian smoothed and each region of reduced conductance (the dark part corresponding to the core) is fitted to a Gaussian. The center of each Gaussian defines a vortex location vector to 0.5 pixel accuracy in the 256×256 pixel images. The averaged vortex lattice basis vectors for a particular image are then transformed to the vortex lattice frame ($\mathbf{z}\|\mathbf{B}$). The vortex lattice vectors, normalized to a_0, at 2.25 kG and $\varphi=7°$ are shown in Fig. 2 in both the surface and vortex frame for a sequence of angles $0° \leq \theta \leq 83°$.

The flux-lattice distortion was determined by fitting the lattice basis vectors to an ellipse. For $\mathbf{B}\|\mathbf{c}$ the six nearest neighbors lie on a circle of unity radius. As the tilt angle increases this circle becomes increasingly elliptical with a semiminor radius of size γ and a semimajor radius of size $1/\gamma$ in the vortex frame. The semiminor axis is roughly aligned with the tilt direction. (An ellipse for the $\theta=70°$ data is plotted in Fig. 2.)

The values of the ellipse fitting parameter $1/\gamma$ for the lowest and highest fields are collected in Fig. 3 for the two in-plane projections $\varphi=7°$ and $\varphi=-21°$. While most of the normalized vortex basis vectors appear to be roughly field independent, the higher field data do systematically show slightly larger values of $1/\gamma$ than the lowest field data. The distortions for the $\varphi=-21°$ are also systematically smaller than those of $\varphi=7°$ case. At fields approaching H_{c1}, one might expect field-dependent corrections to $1/\gamma$ [10]. The simple bulk London model would predict a tilt dependence given by [4,5]

$$\gamma(\theta)=[1+(m_a/m_c)\tan(\theta)]^{1/4}[\cos(\theta)]^{1/2}.$$

A best fit for both in-plane projections at $H_a=5$ kG with mass ratio as the only parameter gives $m_c/m_a=7$ (± 1). For $H=0.5$ kG the ratio is 5.5 (± 1). H_{c2} anisotropy experiments [7] suggest a ratio $m_c/m_a=11$. Our fits are in reasonable agreement with the London model. However, this model may be oversimplified for the case of $2H$-$NbSe_2$ as the Fermi surface is described by an undulating cylinder with considerable nesting and charge-density-wave gaps.

A more serious disagreement arises with this model when one considers the angular orientation of vortices on this "distortion" ellipse. Chains are not observed along the tilt direction as predicted to be the lowest energy state from a bulk uniaxial anisotropic theory [4,5] and as observed in low field decoration experiments. Instead nearest-neighbor vortices are located very close to the semimajor axis of the ellipse, which is at 90° to the tilt direction. In-plane (a,b) anisotropy may play some role in this, since it is responsible for locking of the crystal and flux-lattice orientations when $\theta=0°$, and creating sixfold symmetric vortex cores [11]. If this were the case, by applying the field with an in-plane projection φ that is shifted by 30° from $\varphi=+7°$, one would expect to observe a rather different behavior. Instead, we observe the identical locking of the flux lattice to the semimajor axis orientation of the ellipse for $\varphi=-21°$. Furthermore, the influence of the hexagonal crystalline in-plane anisotropy

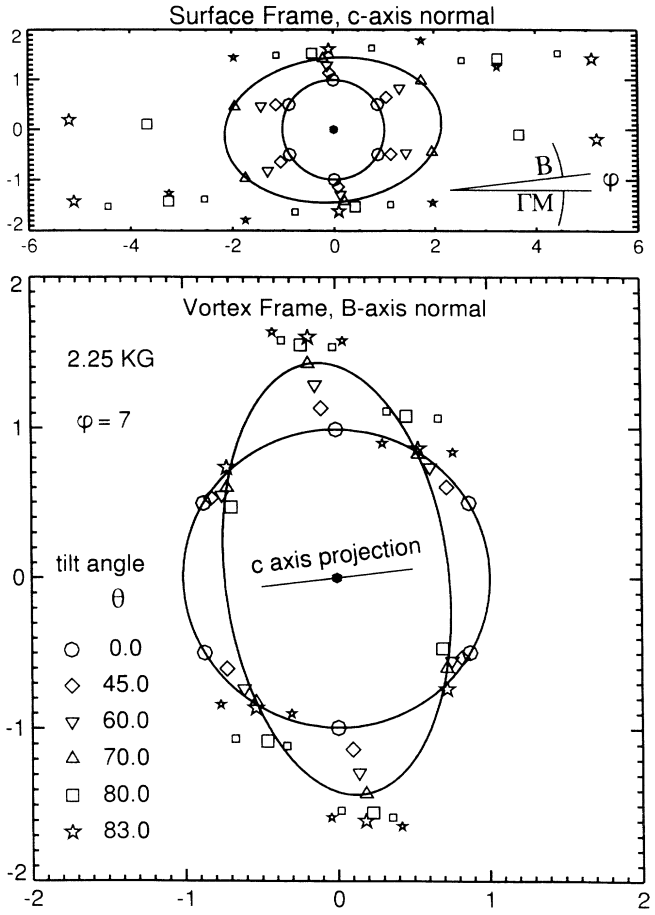

FIG. 2. Vortex basis vectors normalized to a_0 as observed in the surface frame (top) and transformed to the vortex frame (bottom) at different angles indicated by the symbols at the lower left. The averaged basis vectors, large symbols, lie on an ellipse ($\theta=0°$ and $\theta=70°$ are shown), which becomes increasingly elongated with larger θ. At the highest angles (80° and 83°) the buckling instability results in a more complex unit cell. Here smaller symbols show a pair of vortex basis vectors shifted to the left and to the right of the average basis vector.

appears to be rather complicated.

As the tilt angle θ is increased to 80° and beyond the rows of vortices become unstable to undulations, and then undergo at least two distinct transitions to ordered superlattice structures. Two groups [12,13] have predicted instabilities for the distorted hexagonal structure of the flux lattice in uniaxial superconductors at angles greater than 60° for $m_c/m_a \sim 3600$ and 69° for $m_c/m_a \sim 50$. The instabilities that we observe ($\geq 80°$, $m_c/m_a = 6-8$) are consistent with this trend, although calculations have not been done for our case explicitly. In Fig. 1 at 80° a zigzag pattern is observed where the displacement pattern repeats after three vortices (3×1). At 83° another distinct zigzag pattern, that repeats after two vortices (2×1) is visible. The lattice basis vectors along the rows have been plotted in two different ways in Fig. 2. First a direct

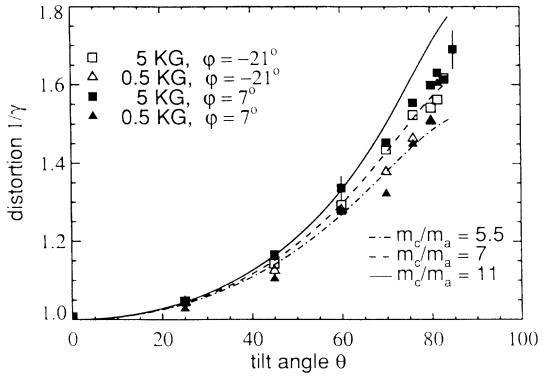

FIG. 3. Normalized semimajor axis length $1/\gamma$ that describes the lattice distortion in the vortex frame (lower part of Fig. 2). The lines indicate predictions of anisotropic London theory for various mass ratios. Our experimental error increases with θ as indicated by the error bars on two points.

average of the split neighbors form the larger points defining the ellipse, used to evaluate γ; the individual split basis vectors for each angle are shown explicitly as well with somewhat smaller symbols. The nearest-neighbor vectors at 4 and 10 o'clock are the only basis vectors that do not suffer from this instability. With increasing θ, the amplitude of these row undulations also increases. By further increasing the tilt to 85° disorder sets in and no discernible lattice structure is evident. This occurs sooner in θ for lower values of field, i.e., 0.5 kG, probably reflecting the dominance of pinning over vortex interactions under these conditions.

In conclusion, we have investigated the structure of the flux lattice on the surface of a uniaxial anisotropic superconductor with STM for numerous tilted magnetic fields. Distortions to the flux lattice spacing in rough agreement with London theory are found (assuming a somewhat reduced mass ratio). The angular orientation of the lattice disagrees with the London result, and indicates some shear in the lattice. For shallow tilt angles various buckling instabilities are observed followed by a disordering transition.

The authors acknowledge useful discussions with V. Kogan, A. Sudbo, and R. Kleiman, and thank D. Grier for the data analysis code.

[1] A. M. Grishin, A. Yu Martynovich, and S. V. Yampol'skii, Zh. Eksp. Teor. Fiz. **97**, 1930 (1990) [Sov. Phys. JETP **70**, 1089 (1990)]; A. I. Buzdin and A. Yu Simonov, Pis'ma Zh. Eksp. Teor. Fiz. **51**, 168 (1990) [JETP Lett. **51**, 191 (1990)].

[2] C. A. Bolle, P. L. Gammel, D. G. Grier, C. A. Murray, D. J. Bishop, D. M. Mitzi, and A. Kapitulnik, Phys. Rev. Lett. **66**, 112 (1991).

[3] P. L. Gammel, D. J. Bishop, J. P. Rice, and D. M. Ginzberg, Phys. Rev. Lett. **68**, 3343 (1992).

[4] L. J. Campbell, M. M. Doria, and V. G. Kogan, Phys. Rev. B **38**, 2439 (1988); L. N. Bulaevskii, M. Ledvij, and V. G. Kogan, Phys. Rev. B **46**, 366 (1992).

[5] K. G. Petzinger and G. A. Warren, Phys. Rev. B **42**, 2023 (1990).

[6] E. M. Forgan, Physica (Amsterdam) **185-189C**, 247 (1991).

[7] P. de Trey, S. Gygax, and J. P. Jan, J. Low Temp. Phys. **11**, 421 (1973).

[8] K. Takita and K. Masuda, J. Low Temp. Phys. **58**, 127 (1984); L. P. Le *et al.*, Physica (Amsterdam) **185-189C**, 2715 (1991).

[9] H. F. Hess *et al.*, Phys. Rev. Lett. **62**, 2519 (1989); H. F. Hess, Physica (Amsterdam) **169B**, 422 (1991).

[10] A. I. Buzdin and A. Yu Simonov, Physica (Amsterdam) 175C, 143 (1991). Assuming a demagnetization factor of 0.95, the misalignment between the applied field H_a and the direction of the induction B in the sample is estimated to be less than 2° for certain angles at 509 G and smaller than 1° for the rest of the data. A sample misalignment of 1° can change the mass ratio by 15%.

[11] H. F. Hess, R. B. Robinson, and J. V. Waszczak, Phys. Rev. Lett. **64**, 2711 (1990); F. Gygi and M. Schluter, Phys. Rev. Lett. **65**, 1820 (1990).

[12] A. Sudbo and E. H. Brandt, Phys. Rev. Lett. **68**, 1758 (1992).

[13] S. T. Chui, Solid State Commun. 83, 441 (1992).

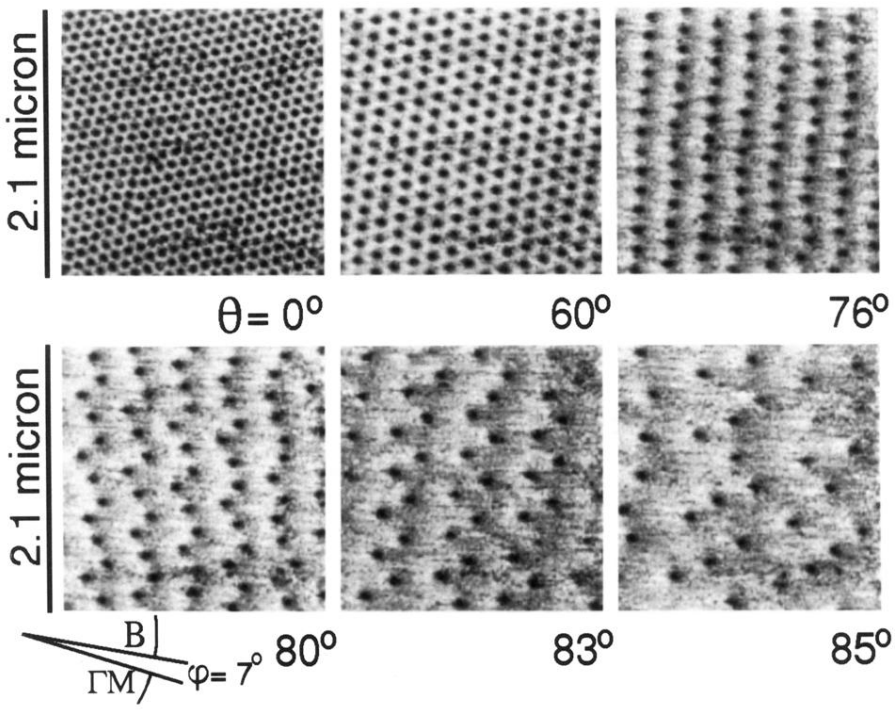

FIG. 1. STM conductance images dI/dV $(x,y,V=1.3$ mV) showing vortex locations on the surface of $2H$-$NbSe_2$ at $\theta=0°$, 60°, and 76° (top row) and 80°, 83°, and 85° (bottom row) where the buckled and disordered phases are evident. The directions of ΓM and the in-plane projection of B are indicated. The applied field is 2.25 kG.